Extraction and Characterization of Silica from Reeds Biomass (*Imperata cylindrical*) in Various Annealing Temperatures

Dyah Ayu Pramoda Wardani,[1*] Neny Kurniawati,[2] Budi Hariyanto,[2] Nazopatul Patonah Har,[3] Noviyan Darmawan,[4,5] Rofikul Umam,[6] Irzaman[3]

[1]*Department of Chemistry, Faculty of Mathematics and Natural Science, University of Palangka Raya, Palangka Raya 73111, Central Kalimantan, Indonesia; dayupwardani@mipa.upr.ac.id*
[2] *Department of Physics, Faculty of Mathematics and Natural Science, University of Palangka Raya, Palangka Raya 73111, Central Kalimantan, Indonesia*
[3] *Department of Physics, Faculty Mathematics and Natural Science, IPB University, Bogor 16680, West Java, Indonesia*
[4] *Department of Chemistry, Faculty Mathematics and Natural Science, IPB University, Bogor 16680, West Java, Indonesia*
[5] *Halal Science Center LPPM IPB, IPB University, Bogor 16680, West Java, Indonesia*
[6] *School of Science and Technology, Kwansei Gakuin University, Japan*

Received December 13, 2022; accepted March 23, 2023; published March 30, 2023

Abstract—Reeds biomass has been successfully extracted. It calcinated with annealing temperatures at 800°C (A800), 850°C (A850), and 900°C (A900). The x-ray pattern showed that it has a cristoballite (SiO_2) crystal structure. The band gap energy values are 3.8 eV, 3.7 eV and 4.7 eV, respectively. FTIR spectra show the groups are silanol, siloxane, and monohydride. Quantitatively, it provides results to determine the optical properties and dielectric functions which indicate a shift to longer wavelengths with an increase in annealing temperature. The morphology presents a different image where the particles are formed flakes (A800), aggregates (A850) and porous aggregates (A900).

Keywords: Reeds biomass, annealing temperature, cristoballite, band gap energy, optical properties, dielectric function

In Indonesia, reeds (*Imperata cylindrica*) are natural vegetation that is very abundant and covers a total of 8.5 million hectares, especially in tropical and subtropical areas. Reeds plants are wild plants and easy to grow and reproduce [1]. Reeds are also known as some of the most difficult to eradicate and harmful pest plants. People use reeds for making briquettes and roofs, but their use is limited [2]. The roots are used as medicine, and the leaves are disposed of as agro-waste. The ash from the leaves of reeds can be used as a material for making silica. Silicon dioxide/Silica (SiO_2) is a crucial ingredient in manufacturing a wide variety of materials [3], such as cement and ceramics [4], textiles [5], films [6], paper [7], rubber [8], tires [9]. In this study, we annealed reeds biomass with various annealing temperatures. Annealing is a heat treatment process that changes the physical and sometimes also the chemical properties of a material to increase ductility and reduce the hardness to make it more workable [3], [10], [11].

Figure 1 shows the XRD patterns of annealed reeds biomass at A800, A850, and A900. Qualitative analysis using *Match!* software confirms that the XRD patterns are SiO_2 (cristoballite) (ICDD#96-900-8230). An increase in annealing temperature causes a slight shift in the peak position, addition of peaks, and sharper peak, marked by the values of 2θ (see the data in Table 1).

The band gap energy is calculated using the Direct Tauc plot method. It determines the optical band gap by looking at a linear graph of the relationship E (eV) on the *x*-axis and $(ahv)^{1/m}$ *y*-axis. In Fig. 2, the temperature increase from A800 to A850 shows the decrease of band gap energy values from 3.8 eV to 3.7 eV, and at A900, it increases significantly to 4.7 eV. This shift occurs because a higher annealing temperature can produce higher electron excitation from the valence band to the conduction band as a direct transition.

Figure 3 shows the FTIR spectra of annealed reeds biomass at A800, A850, and A900, the functional groups are indicated by numbers and summarized in Table 2. The functional groups that appear are Si–O–Si, Si–Si, Si–O, –OH, H–Si–Si–H, and Si–OH.

The FTIR pattern was used to determine the optical properties and dielectric function for the firm peaks at the wavenumbers (ω) from 400 to 550 cm^{-1} [12]. For these purposes, Kramers−Kronig's (KK) relation is used in the quantitative analysis of the FTIR pattern. The FTIR spectra were used for determining the refractive index (n), extinction coefficient (k) are shown in Fig. 4(a). The lower intersection wavelength point between $n(\omega)$ and $k(\omega)$ is the transverse optical (T_o) mode, and the higher one is the longitudinal optical (L_o) phonon vibration mode. The

values of T_o and L_o serve in Table 3. The values of T_o generally increase with the increasing of annealing temperature, and the values of Lo at A900 significantly increase because the increasing of annealing temperature can produce higher vibration.

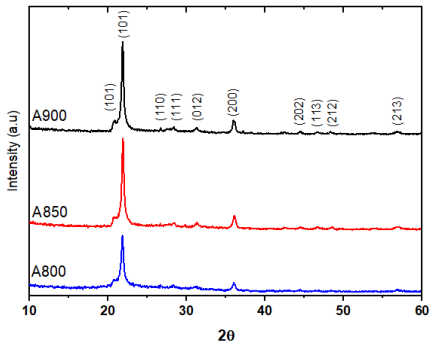

Fig. 1. X-ray diffractograms of annealed reeds biomass at A800, A850, and A900.

Table 1. The XRD data of annealed reeds biomass.

Annealed Reeds Biomass					
A800		**A850**		**A900**	
2θ	*hkl*	2θ	*hkl*	2θ	*hkl*
21.71	101	21.81	101	20.67	101
26.11	110	28.31	111	21.81	101
28.21	111	31.31	012	27.81	110
31.11	012	36.01	200	28.11	111
35.91	200	42.51	211	31.11	012
37.41	112	44.41	202	36.01	200
44.41	202	46.51	202	46.51	202
56.91	213	48.41	113	48.31	113
		49.61	212	49.41	212
		56.71	213	56.81	213

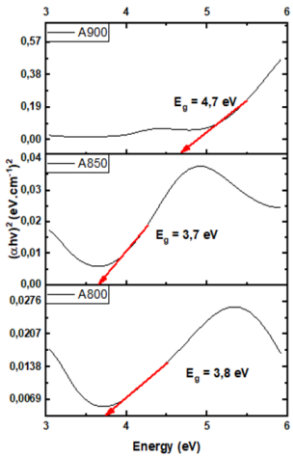

Fig. 2. The band gap energy of annealed reeds biomass.

The dielectric functions for the real part $\varepsilon_1(\omega)$ and imaginary part $\varepsilon_2(\omega)$ in Fig. 4(b) indicate by peaks in the range from 430 to 450 cm^{-1}, it means that at the surface layer, the breaking of the interatomic bonding happens, and a new structure is formed. $\Delta(L_o–T_o)$ is the distance between two optical phonon modes, which increases on increasing annealing temperature as presented in Table 3, probably due to a less stable structure and nonuniformity of lattice in the annealed reeds biomass [13–14].

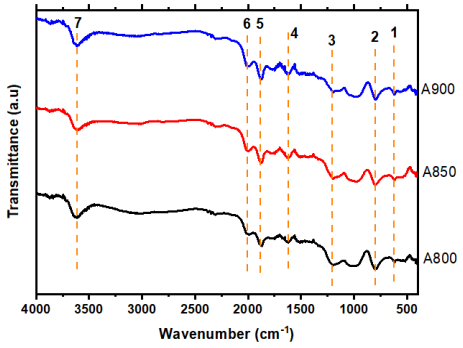

Fig. 3. The FTIR spectra of annealed reeds biomass.

Table 2. The Functional Groups and Wavenumber of Annealed Reeds Biomass

No	Functional Groups	Wavenumber (cm^{-1})		
		A800	**A850**	**A900**
1	symmetric stretching vibration of Si–O [15]	617.221	617.221	619.149
2	Si–Si, Si–O stretching vibration [16]	798.529	796.601	798.529
3	Asymmetric stretching vibration of Si–O [16]	1195.865	1197.794	1195.865
4	–OH bending vibration of Si–OH [17]	1620.205	1620.205	1620.205
5		1867.093	1874.809	1874.809
6	H–Si–Si–H [18]	1990.538	1992.466	2002.111
7	–OH stretching vibration of Si–OH [19]	3614.601	3612.672	3614.601

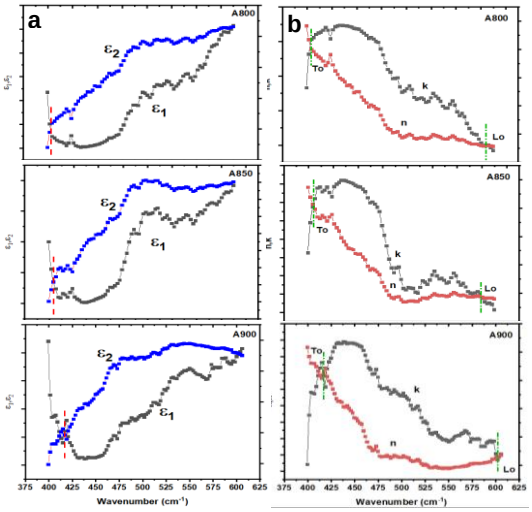

Fig. 4. (a) The optical properties (b) The dielectric function of annealed reeds biomass.

Figure 5 shows the morphology of annealed reeds biomass at A800, A850, and A900 with magnification (a) 2500× and (a) 5000×. The particle with magnification 2500× (Fig. 5(a) A800) shows an irregular flakes form, aggregates form (Fig. 5(a) A850) and porous aggregates form (Fig. 5(a) A900). Then, magnification 5000× in Fig. 5(b) A800, A850, and A900 clearly represent that the increasing of annealing temperature causes a pores form on the surface of reeds biomass particles.

Table 3. Transverse optical phonon (To) and longitudinal optical phonon (Lo), and the real (ε_1) and imaginary parts (ε_2) of the dielectric function from the quantitative analysis of the FTIR spectra in Figure 4 (a) and (b).

Samples	T_o (cm^{-1})	L_o (cm^{-1})	$\Delta(L_o-T_o)$ (cm^{-1})	ε_1, ε_2 (cm^{-1})
A800	403.122	538.139	135.017	403.122
A850	403.122	540.068	136.946	405.051
A900	416.624	601.790	185.166	416.624

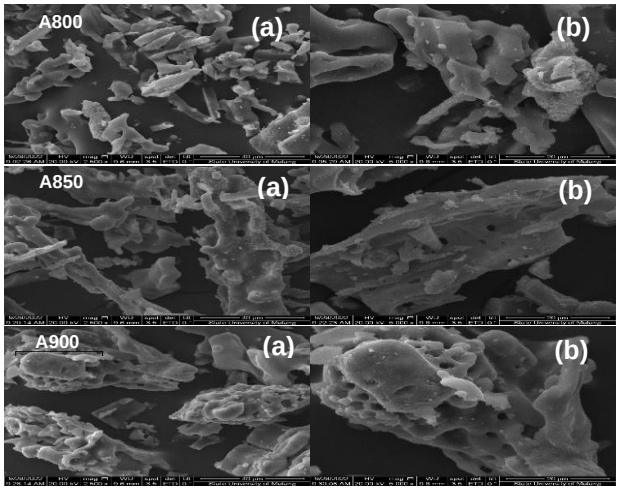

Fig. 5. The morphology result of annealed reeds biomass at A800, A850, and A900 with magnification (a) 2500× and (b) 5000×

This research was funded by PKPT Grant (No. 305/UN24.13/PL2022) by the Ministry of Education and Culture, Research and Technology of the Republic of Indonesia (Kementerian Pendidikan dan Kebudayaan, Riset, dan Teknologi Republik Indonesia).

References

[1] A.F. Ramdja, R.A. Silalahi, N. Sihombing, J. Tek. Kim. **17**(2), 42 (2010).
[2] Z.S. Osvaldo, P. Putra, M. Faizal, J. Tek. Kim. **18**(2), 52 (2012).
[3] I.S. Naji, N.A. Khalifa, H.M. Khalaf, Dig. J. Nanomater.: Biostructures **12**, 899 (2017).
[4] M. Sahri, A.R. Tualeka, N. Widajati, Indian J. Public Heal. Res. Dev. **10**, 601 (2019).
[5] A. Berendjchi, R. Khajavi, M.E. Yazdanshenas, Int. J. Green Nanotechnol. **1**, 1943089213506814 (2013).
[6] P.Y. Steinberg *et al*., Front. Mater. **8,** 27 (2021). doi: https://doi.org/10.3389/fmats.2021.628245.
[7] A.F. Lourenço, J.A.F. Gamelas, J. Sequeira, P.J. Ferreira, J.L. Velho, Bioresources **10**, 8312 (2015).
[8] S. Begum, M. Allaudin, M.A. Qaiser, F. Khan, J. Chem. Soc. Pakistan **21**, 83 (1999).
[9] N.H.N.A. Hadi, A. Anuar, R.K. Shuib, J. Eng. **15**, 71 (2019).
[10] K. Kayed, D.B. Kurd, Silicon **14**, 5157 (2021).
[11] F. Ravaux, N.S. Rajput, J. Abed, L. George, M. Tiner, M. Jouiad, RSC Adv. **7**, 32087 (2017).
[12] H. Liu *et al*., Appl. Surf. Sci. **495**, 143590 (2019).
[13] M. Ghasemifard, E. Fathi, M. Ghamari, Mater. Sci. Semicond. Process. **42**, 349 (2016).
[14] X. Lu *et al*., Ultrason. Sonochem. **55**, 135 (2019).
[15] E.W. Juni, A. Arnelli, S. Sriatun, J. Kim, Sains dan Apl., **15**, 24 (2012).
[16] F. Adam, K. Kandasamy, S. Balakrishnan, J. Colloid Interface Sci. **304**, 137 (2006).
[17] K.C. Wong, J. Chem. Educ. **92**, 1602 (2015).
[18] L.H. Abuhassan, Sains Malaysiana **39**, 837 (2010).
[19] U. Kalapathy, A. Proctor, J. Shultz, J. Chem. Technol. Biotechnol. **75**, 464 (2000).

